



HAL
open science

Simultaneous mass and heat transfer in a biodegradable bio-sourced thermal insulating material

Essolé Padayodi, Mohammad Aghahadi, Said Abboudi, Seyed Amir Bahrani, Rija Raoelison

► **To cite this version:**

Essolé Padayodi, Mohammad Aghahadi, Said Abboudi, Seyed Amir Bahrani, Rija Raoelison. Simultaneous mass and heat transfer in a biodegradable bio-sourced thermal insulating material. Colloque InterUT Systèmes sûrs et durables, Université de Technologie de Compiègne [UTC], Feb 2023, Paris, France. hal-04015659

HAL Id: hal-04015659

<https://hal.science/hal-04015659>

Submitted on 6 Mar 2023

HAL is a multi-disciplinary open access archive for the deposit and dissemination of scientific research documents, whether they are published or not. The documents may come from teaching and research institutions in France or abroad, or from public or private research centers.

L'archive ouverte pluridisciplinaire **HAL**, est destinée au dépôt et à la diffusion de documents scientifiques de niveau recherche, publiés ou non, émanant des établissements d'enseignement et de recherche français ou étrangers, des laboratoires publics ou privés.

Simultaneous mass and heat transfer in a biodegradable bio-sourced thermal insulating material

Essolé PADAYODI^{1*}, Mohammad AGHAHADI^{1,2}, Saïd ABOUDI², S. Amir BAHRANI³, Rija Nirina RAOELISON²

¹Pôle ERCOS, ELLIADD (EA. 4661) –University of Technology of Belfort-Montbéliard, 90010 Belfort, France

²ICB, UMR 6303, CNRS –University of Technology of Belfort-Montbéliard, 90010 Belfort, France

³Institut Mines-Télécom Lille-Douai, University of Lille, Lille, France

Corresponding author: essole.padayodi@utbm.fr

Abstract

Unlike hydrophobic materials, heat transfer in a hydrophilic material in a wet atmosphere is accompanied by mass transfer. This study deals with the thermal metrology of hydrophilic versus hydrophobic materials. An experimental approach based on the asymmetric hot plate method and a theoretical approach of coupled heat and humidity transfers are performed. The experimental results show that, at 20 °C, the thermal conductivity λ of flax fibers insulators increases up to 20% when the relative humidity RH increases from 30% to 90%, i.e. from 0.028 ± 10^{-3} to 0.033 ± 10^{-3} W.m⁻¹.K⁻¹ while λ remains constant for the hydrophobic material. This agrees with the theoretical model results.

Keywords: *bio-sourced materials, thermal conductivity, coupled transfer, hot plate method, hydrophilic insulators.*

I. INTRODUCTION

Thermal insulators made of bio-sourced materials are being increasingly developed to cut greenhouse gas emission in building insulation. However, despite their interest, bio-sourced insulators have a major disadvantage related to their behavior in relation to moisture as they are high hydrophilic materials. The classical models of thermal metrology do not match with these materials.

Indeed, firstly there are different methods for measuring the thermal conductivity of a material. These include the guarded hot plate [1], flash [2], "Hot disc" [3], hot wire, hot ribbon, tri-layer [4], hot plate methods [5, 6], etc. Among these, the tri-layer and hot plate methods are more suitable for characterizing low thermal conductivity materials such as bio-sourced materials [5, 6] or super insulating materials [6].

Secondly, in the case of hydrophilic materials, such as bio-sourced materials, the measurement of thermal conductivity cannot be carried out with precision without a necessary consideration of the simultaneous transfer of heat and humidity [7].

The objective of this study is to develop a centered hot plate device considering the humidity influence so to allow a measurement of the thermophysical properties of a hydrophilic material in a humid environment.

II. EXPERIMENTAL APPROACH

A. Water sensitive and non-sensitive media

The hydrophilic vs hydrophobic distinction is justified when coupled heat-humidity transfer is characterized. The experimental approach is thus performed on a hydrophilic insulator based flax fibers (LFB) (Fig. 1a) made of random distributed and compressed $\varnothing 20$ μ m fibers (Fig.2) and on a hydrophobic material made of a phase change polymer (PCM) (*Rubitherm[®] paraffin*) (Fig; 1b) with solidification temperature about 27 °C.

The contact angles of LFB and PCM measured by the droplet analysis are respectively $\theta_{PCM} = 112^\circ \pm 2^\circ$ and $\theta_{LFB} = 78^\circ \pm 2^\circ$ (Fig. 1c and 1d), showing that the surface of LFB media is wettable (as $\theta_{LFB} < 90^\circ$) while the PCM surface is non-wettable (as $\theta_{PCM} > 90^\circ$). The latter is hydrophobic and the FLB media is hydrophilic and could uptake the ambient humidity [8, 9, 10]. This is confirmed by the water uptake test. The Fig. 3 plots the evolution of the water content of the LFB sample for different relative humidity HR of the ambient air.

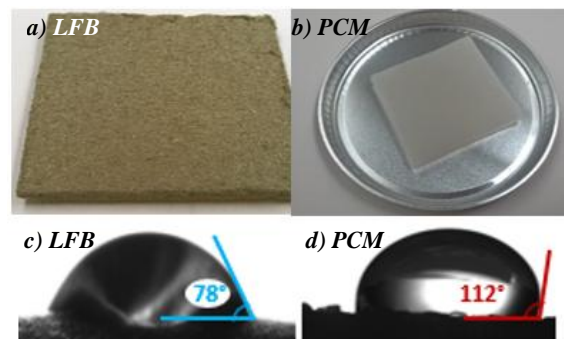


Figure 1. Contact angle (water droplet) on the PCM and the LFB samples

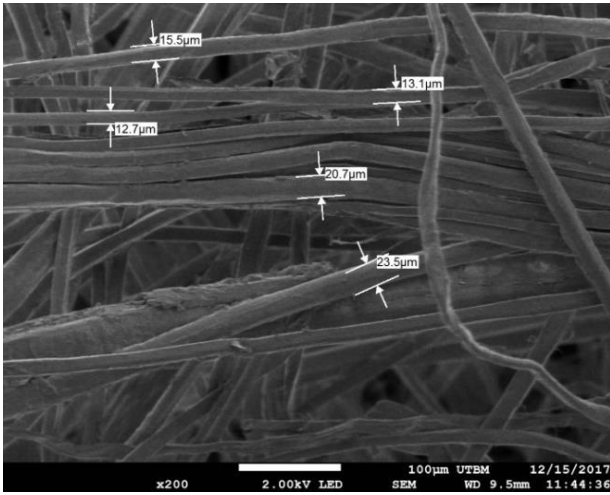


Figure 2. MEB analysis of LFB samples

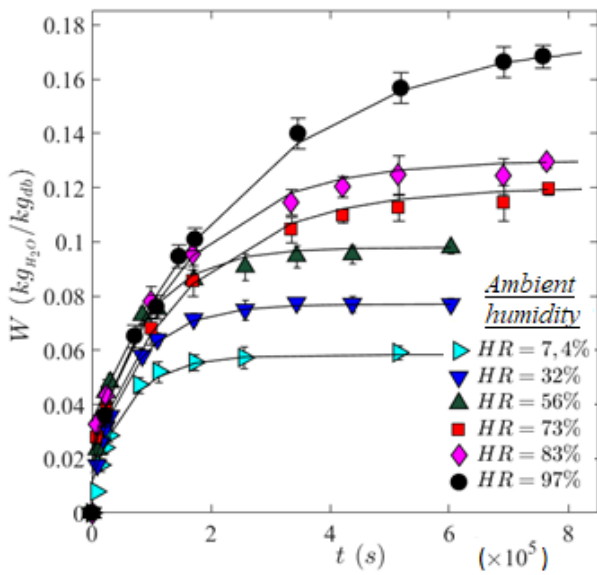


Figure 3. Variation of the water content of the LFB sample in atmospheres at variable relative humidity

Clearly, the material LFB can absorb until 17 % wt of the humidity when lying in an ambient air at 97% HR. Biosourced materials are high hydrophilic, as the result, coupling heat and humidity transfer is required when applying thermal metrology to biobased insulators.

B. Device for thermal conductivity measurement

An "asymmetrical centered hot plate" device [11, 12] was used to measure the thermal conductivity of the studied samples. It consists of (Fig. 4) a 21 Ω flat heating element of 46 × 46 mm² and 0.15 μm thickness (*Omega*[®], *KHLV-202/10-p*) which is inserted between the sample to characterize and a

reference sample with a well-known thermal conductivity ($\lambda_2 = 0.069 \text{ W.m}^{-1}.\text{K}^{-1}$). Samples are compressed (pressure $\approx 6 \times 10^{-2} \text{ MPa}$) between two identical aluminum blocks. K-type thermocouples record the evolution of interfaces temperatures $T_c(t)$, $T_o(t)$ and $T_1(t)$ (Fig. 4). The heating element is connected to a power supply (*AIM-TTI*[®], *PLH250-P*, *UK*) and thermocouples are connected to an acquisition unit (*Omega*[®], *TC-08*, *UK*).

The test is carried out on low-thickness samples ($\approx 4 \text{ mm}$) so to allow a unidirectional heat flux across the sample, from one side to the other, and to minimize the lateral heat losses. The hot plate device provided with samples is arranged in the climate Chamber (Fig. 5) so to set the ambient atmosphere at a given temperature and humidity.

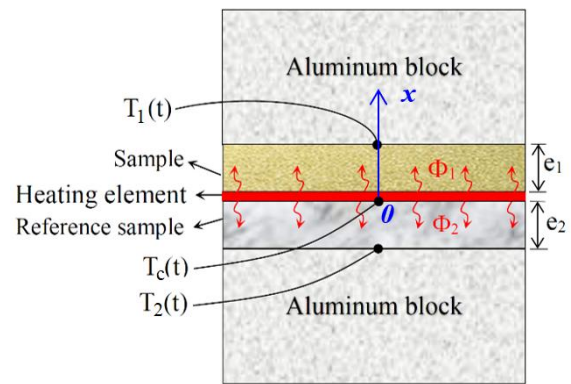


Figure 4. Schematic layout of the "asymmetrical centered hot plate"

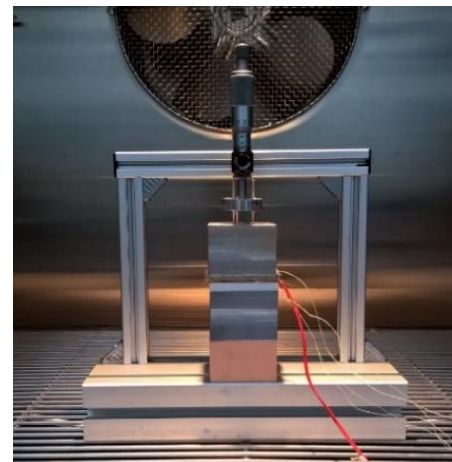


Figure 5. Experimental device of "asymmetrical centered hot plate" arranged in a climatic chamber.

C. Measuring protocol

When a voltage ($U = 2.33 \pm 0.01 \text{ V}$) and a current ($I = 0.11 \pm 0.01 \text{ A}$) is applied, a heat flow ($\phi = U^2/R.S$) is generated

through samples. The interface temperatures $T_c(t)$, $T_1(t)$ and $T_2(t)$ are then recorded until stationary regime (after about 3h). By neglecting the lateral heat loss, the generated flux (ϕ) is the sum of both heat fluxes ϕ_1 and ϕ_2 , passing through each sample:

$$\phi = \phi_1 + \phi_2 \quad (1)$$

In a stationary regime, the Fourier's law of heat conduction allows us to write :

$$\begin{cases} \phi_1 = \frac{\lambda_1}{e_1} (T_c - T_1) \\ \phi_2 = \frac{\lambda_2}{e_2} (T_c - T_2) \end{cases} \quad (2)$$

The thermal conductivity λ_1 of the sample is deduced from the above equations as follow :

$$\lambda_1 = \frac{e_1}{T_c - T_1} \left[\frac{U^2}{RS} - \frac{\lambda_2}{e_2} (T_c - T_2) \right] \quad (3)$$

For the LFB sample, measurements are undertaken at relative humidity conditions of 30%, 50%, 70% and 90% RH, the temperature being maintained for each RH case at 20 °C, 30°C, 40 °C and 50 ° C. For the PCM sample, measurements are performed at extreme RH of 30% and 90% and at 10°C and 15 °C, i.e, below the phase change temperature of PCM (27°C).

D. Experimental determination of thermal capacity and absolute density

As the thermal capacity and the absolute density are involved in the coupled heat-humidity transfers, these parameters are previously measured on the LFB and PCM samples. The density is determined by the hydrostatic weighing method using a balance and the thermal capacity is measured by the continuous temperature programming method using the DSC calorimeter (*TA Instrument®*, *Q20, USA*), as well detailed in our previous paper [13]. The thermal capacity of the sample c_{p_e} is then calculated from the correlation :

$$c_{p_e}(T) = c_{p_r}(T) \frac{\phi_e - \phi_b}{\phi_r - \phi_b} \frac{m_r}{m_e} \quad (4)$$

Where C_{p_r} , m_r and ϕ_r are respectively the thermal capacity, the mass and the thermal flux of the reference sample, m_e and ϕ_e , the mass and the thermal flux of the sample to be characterized and ϕ_b the thermal flux of the empty sample holder.

Experimental results of C_{p_e} are plotted on Fig. 6.

III. THEORETICAL APPROACH OF COUPLED HEAT AND HUMIDITY TRANSFERS

A. Analytical model of coupled heat-humidity transfers

When a heat source is applied to a hydrophilic media lying in a humid atmosphere, heat and moisture transfer phenomena occur simultaneously through this medium. The present study proposes a coupled heat and humidity transfer model that will be compared to the permanent hot plate measurement method applied to a porous sample within a humid atmosphere.

As the heat transfer can be assumed to be unidirectional at the center of the sample, according to Ox direction (Fig. 4), the coupled heat-humidity transfer can be considered as a one-dimensional problem.

The moisture and heat balance equations are then:

- *Mass balance (liquid and vapor phases):*

$$\rho_0 \frac{\partial X_l}{\partial t} = \frac{\partial}{\partial x} \left[\rho_0 \left(D_X^l \frac{\partial X_l}{\partial x} + D_T^l \frac{\partial T}{\partial x} \right) \right] - \dot{m} \quad (5)$$

$$\rho_0 \frac{\partial X_v}{\partial t} = \frac{\partial}{\partial x} \left[\rho_0 \left(D_X^v \frac{\partial X_v}{\partial x} + D_T^v \frac{\partial T}{\partial x} \right) \right] + \dot{m} \quad (6)$$

where D_X^l and D_X^v are isothermal mass diffusivity of liquid phase and of vapor phase respectively ($m^2 s^{-1}$) and D_T^l and D_T^v are non-isothermal mass diffusivity of liquid phase and vapor phase respectively ($m^2 s^{-1} K^{-1}$) and T , the temperature, X , the water content and \dot{m} , the quantity of evaporated water per unit of sample volume and per unit of time.

By summing both equations, the total mass balance of the two phases is :

$$\frac{\partial X}{\partial t} = \frac{\partial}{\partial x} \left[\left(D_X \frac{\partial X}{\partial x} + D_T \frac{\partial T}{\partial x} \right) \right] \quad (7)$$

$$\text{where } D_X = D_X^l + D_X^v \text{ and } D_T = D_T^l + D_T^v \quad (8)$$

In the vapor phase, by neglecting the accumulation term over the transport term, \dot{m} becomes :

$$\dot{m} = - \frac{\partial}{\partial x} \left[\rho_0 \left(D_X^v \frac{\partial X_v}{\partial x} + D_T^v \frac{\partial T}{\partial x} \right) \right] \quad (9)$$

As the thermal diffusion can be neglect over the mass diffusion ($D_T^v \ll D_X^v$), \dot{m} becomes :

$$\dot{m} = - \frac{\partial}{\partial x} \left(\rho_0 D_X^v \frac{\partial X_v}{\partial x} \right) \quad (10)$$

- *Heat balance*

On a macroscopic scale, by neglecting the kinetic energy and the assumption that water adsorbed in the pores is not a separate phase and by introducing the heat capacity at constant pressure, the equation of energy is :

$$\rho C_p^* \frac{\partial T}{\partial t} = \frac{\partial}{\partial x} \left[\lambda^* \frac{\partial T}{\partial x} + \rho_0 D_X^v L_v \frac{\partial X_v}{\partial x} \right] \quad (11)$$

Where λ^* and C_p^* are respectively the apparent thermal conductivity and heat capacity of the sample and L_v , the latent heat of vaporization estimated as:

$$L_v = 2495 - 2.346 T \quad (12)$$

- The initial and boundary conditions, referring Fig. 4, are defined as :

$$\text{At } t = 0, \begin{cases} X = X_i \\ T = T_i \end{cases} \quad (13)$$

$$\text{At } t > 0 \text{ and } x = 0, \begin{cases} \frac{\partial X_i}{\partial x} = 0 \\ -\lambda \frac{\partial T}{\partial x} = \phi \end{cases} \quad (14)$$

$$\text{At } t > 0 \text{ and } x = e_1, \begin{cases} \frac{\partial X_i}{\partial x} = 0 \\ T = T_i \end{cases} \quad (15)$$

X_i and T_i in eq. 13 are respectively the equilibrium water content and the temperature of the sample with the climatic chamber atmosphere.

The eq. 15 implies that the mass transfer flux is null at the sample and the aluminum block interface and is assumed to be isothermal over time.

B. FE modeling of coupled heat-humidity transfers

A finite elements (FE) simulation using COMSOL Multiphysics[®] software is implemented to solve equations 7 and 11 with the associated boundary conditions 13, 14 and 15. Tables 1 gives the experimental and literature values of parameters involved in the mathematical and in the FE simulations.

TABLE I. THERMOPHYSICAL PROPERTIES (ρ_0 , C_p^* , X_i AND λ ARE EXPERIMENTALLY MEASURED WHILE THE ISOTHERMAL MASS DIFFUSIVITY ON VAPOR PHASE IS AVERAGE VALUES OF BIOSOURCED MATERIALS FROM LITERATURE)

		Density	Thermal capacity	Thermal conduct.	Mass diffusion	Water content
		ρ_0	C_p^*	λ	D_X^v	X_i
		($Kg.m^{-3}$)	($J.Kg^{-1}.K^{-1}$)	($W.m^{-1}.K^{-1}$)	($m^2.s^{-1}$)	----
LFB sample	$T_i=30^\circ C / HR=30\%$	988	1660	0.030	2.78×10^{-9}	0.08
	$T_i=40^\circ C / HR=90\%$	988	1524	0.039	4.65×10^{-10}	0.17
PCM sample	$T_i=10^\circ C / HR=90\%$	867	1038	0.201	---	---
	$T_i=15^\circ C / HR=90\%$	867	2676	0.217	---	---

IV. RESULTS AND DISCUSSION

A. Thermophysical characteristics

Figure 6 plots the thermal capacity C_{p_e} values of LFB and PCM samples measured experimentally. The thermal capacity of LFB decreases slightly (from $2245 \pm 20 J.Kg^{-1}.K^{-1}$ at $5^\circ C$ to $1365 \pm 20 J.Kg^{-1}.K^{-1}$ at $50^\circ C$) while the thermal capacity of PCM is growing significantly around the phase change temperature, i.e. $27^\circ C$, followed by a decreasing.

The experimental values of the thermal conductivity λ of the LFB sample measured with the hot plate device at different temperatures and for different relative humidity are plotted on Fig. 7. Table 2 shows the thermal conductivity measured on the PCM materials.

Results of Figure 7 show that the thermal conductivity of the hydrophilic material LFB increases as the temperature increases (+ 22% when the temperature increases from $20^\circ C$ to $50^\circ C$). In addition, as moisture increases (from 30% to 90% RH), the thermal conductivity is increased (from $0.028 \pm 10^{-3} W.m^{-1}.K^{-1}$ to $0.033 \pm 10^{-3} W.m^{-1}.K^{-1}$ at $20^\circ C$). Clearly, the humidity transfer contributes to the heat transfer.

Regarding the PCM material, the thermal conductivity increases with the temperature, as might be expected. In an

atmosphere at 30% RH, it increases for example from $0.198 \pm 10^{-3} W.m^{-1}.K^{-1}$ at $10^\circ C$ to $0.219 \pm 10^{-3} W.m^{-1}.K^{-1}$ at $15^\circ C$ (i.e. + 10% increasing). On the other hand, it hardly increases between two extreme values of humidity (λ increases less than 2% when the relative humidity increases from 30% RH to 90% RH) corroborating thus the inaction of moisture on hydrophobic materials.

These results confirm the necessity to consider the coupled heat and moisture transfer when measuring thermophysical characteristics of hydrophilic materials.

The experimental values of the thermal conductivity of PCM samples measured using the hot plate have been compared to the measurements performed with a commercial apparatus (*TA Instrument[®], DTC 300, USA*). The results given by the commercial apparatus showed a low difference (< 2%) with those measured with the hot plate device. The latter is then validated.

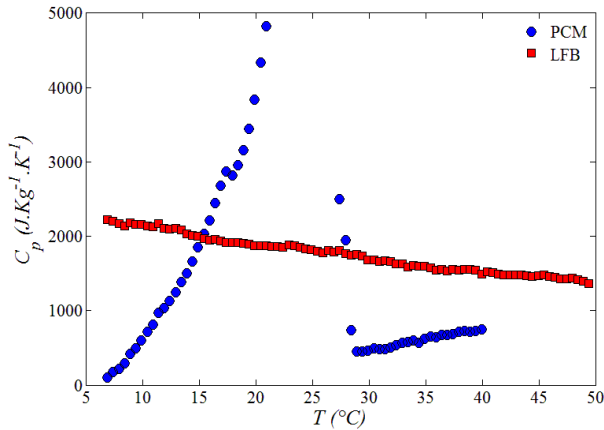


Figure 6: Variation of the heat capacity of PCM and LFB materials according to temperature

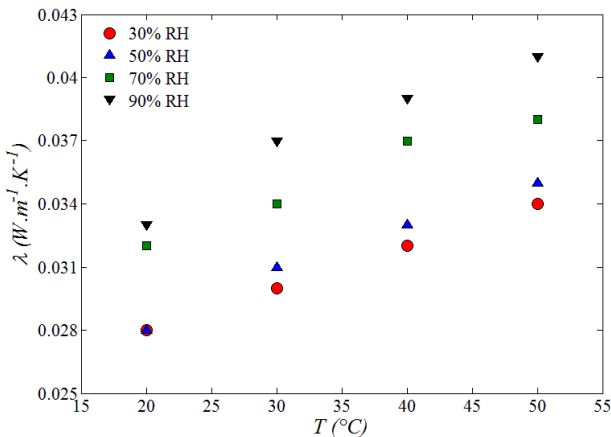


Figure 7 : Thermal conductivity variation of the LFB material as a function of temperature for different relative humidity.

TABLE II. THERMAL CONDUCTIVITY OF THE PCM MATERIAL AT DIFFERENT TEMPERATURES T_i AND RELATIVE HUMIDITY

Initial temperature	Relative humidity RH	
	HR= 30%	HR= 90%
at $T_i=10^\circ\text{C}$	0.198	0.201
at $T_i=15^\circ\text{C}$	0.219	0.217

B. Numerical results

First, to verify the assumption of a unidirectional heat transfer in the center of the sample when arranged in the hot plate, the heat fluxes ϕ_x , ϕ_y and ϕ_z according to Ox , Oy and Oz directions given by the FE modeling at the center of the sample are compared on Fig. 8. As one can see, the heat fluxes ϕ_y and ϕ_z are almost null while the heat flux ϕ_x increases up to $27 \text{ W}\cdot\text{m}^{-2}$ when the hygro-thermal equilibrium is

established. This validates the unidirectional heat transfer hypothesis

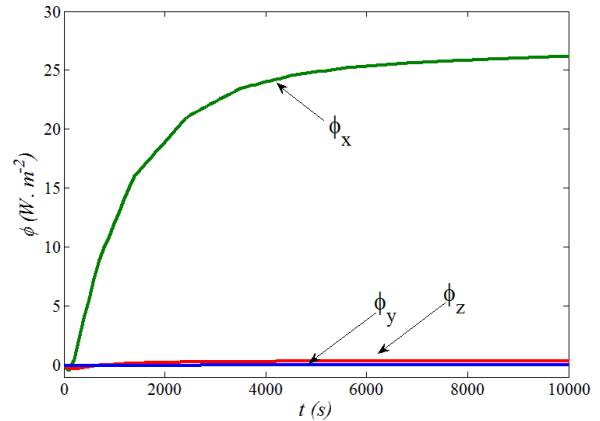


Figure 8 : Heat flux variation computed by COMSOL Multiphysics.

Figures 9 and 10 show a comparison between the experimental and calculated temperatures $\Delta T(t) = T_o(t) - T_i$ on the rear face of the PCM and LFB samples, respectively. In the case of hydrophobic material, the latent heat of vaporization L_v is considered nil, thus the coupling term in the coupled system of equation 11 is canceled. The equation becomes a simple heat transfer problem.

In both cases, a good correlation was observed between the experimental and the numerically simulated curves (variance not exceeding 2%). One can so consider that the proposed coupled heat-moisture transfer model is validated.

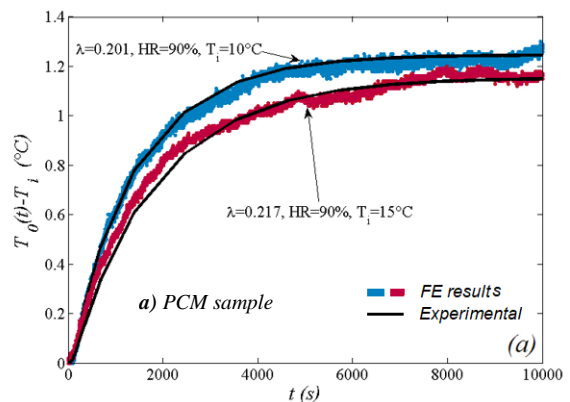


Figure 9: Comparing of the experimental and the calculated temperatures on the rear face of the PCM sample

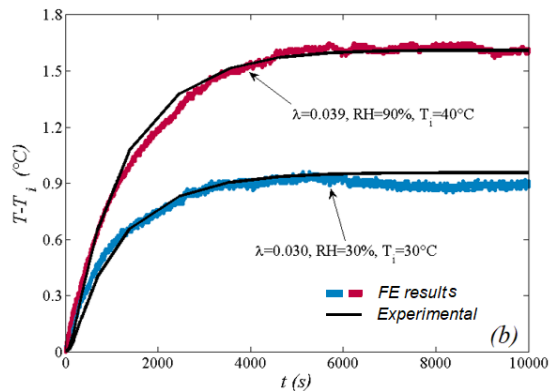


Figure 10: Comparing of the experimental and the calculated temperatures on the rear face of the LFB sample

V. CONCLUSION AND PERSPECTIVES

The increase of thermal insulators based on hydrophilic biosourced materials for building insulation needs implies to develop required models of coupled heat and humidity transfers for these materials' characterization. In this study, a bio-sourced and a phase change material are respectively considered as a hydrophilic and hydrophobic medium. Humidity adsorption and contact angle investigation confirm the choice of these samples. Then, the coupled heat and moisture transfer are modeled in 1D Cartesian coordinate by neglecting the mass transfer through the liquid phase. COMSOL Multiphysics® helps us to validate the unidirectional heat transfer hypothesis. In addition, this mathematical model has been solved with this software. The results show a good agreement between the numerical and experimental approaches with a deviation of less than 2%.

The asymmetric hot plate method is then used to measure the thermal conductivity of these materials in humid atmospheres. At least three measurements are realized in stationary regime. The results show that moisture affects the thermal conductivity of the bio-sourced material while it has no effect on the thermal conductivity of the PCM material.

REFERENCES

- [1] T. Kobari, J. Okajima, A. Komiya, S. Maruyama, "Development of guarded hot plate apparatus utilizing Peltier module for precise thermal conductivity measurement of insulation materials", *Int. J. Heat Mass Transf.*, vol. 91, 2015, pp.1157–1166.
- [2] A. Degiovanni, M. Laurent, "Une nouvelle technique d'identification de la diffusivité thermique pour la méthode « flash »", *Rev. Phys. Appliquée*, vol. 21, 1986, pp. 229–237.
- [3] Y. Jannot, Z. Acem, "A quadrupolar complete model of the hot disc", *Meas. Sci. Technol.*, vol. 18, n°5, 2007, pp. 1229–1234.

- [4] S.A. Bahrani, Y. Jannot, A. Degiovanni, "Extension and optimization of a three-layer method for the estimation of thermal conductivity of super-insulating materials", *J. Appl. Phys.*, vol. 116, n°14, 2014.
- [5] Y. Jannot, V. Felix, A. Degiovanni, "A centered hot plate method for measurement of thermal properties of thin insulating materials", *Meas. Sci. Technol.*, vol. 21, 2010, 035106.
- [6] V. Félix, "Caractérisation Thermique de Matériaux Isolants Légers Application à des Aérogels de Faible Poids Moléculaire". Ph.D. thesis, nov. 2011.
- [7] H. Bal, Y. Jannot, N. Quenette, A. Chenu, S. Gaye, "Water content dependence of the porosity, density and thermal capacity of laterite-based bricks with millet waste additive", *Constr. Build. Mater.*, vol. 31, 2012, pp.144–150.
- [8] K-E. Atcholi, E. Padayodi, J-C. Sagot, T. Beda, O. Samah, J. Vantomme, "Thermomechanical behavior of the structures of tropical clays from Togo (West Africa) fired at 500 °C, 850 °C and 1060°C", *Constr. Build. Mater.*, vol. 27, 2012, pp. 141–148.
- [9] D. Quéré, "Les surfaces super-hydrophobes", *Images de la Phys.*, 2005, pp. 239–244.
- [10] K-E. Atcholi, E. Padayodi, J. Vantomme, K. Kadja, D. Perreux, "Experimental study of the drying and modelling of the humidity migration in a clay matrix", *Int. J. Simul. Multidisci. Des. Optim.*, vol. 2, n°1, 2008, pp. 91–97.
- [11] N. Laaroussi, A. Cherki, M. Garoum, A. Khabbazi, A. Feiz, "Thermal properties of a sample prepared using mixtures of clay bricks", *Energy Procedia*, vol. 42, 2013, pp. 337–346.
- [12] Y. Jannot, A. Degiovanni, V. Grigorova-Moutiers, J. Godefroy, "A passive guard for low thermal conductivity measurement of small samples by the hot plate method", *Meas. Sci. Tech.*, vol 28, 2017, pp. 15008
- [13] M. Aghahadi, E. Padayodi, S. Abboudi, S.A. Bahrani, "Physical modeling of heat and moisture transfer in wet bio-sourced insulating materials", *Review of Sci. Inst.*, vol. 89, 104902, 2018.